SENSITIVITY TO BASIS MISMATCH IN COMPRESSED SENSING

Yuejie Chi[†]*, Ali Pezeshki*[‡]*, Louis Scharf*[‡] *and Robert Calderbank*[†]

[†]Princeton University
Department of Electrical Engineering
Princeton, NJ 08544, USA

[‡]Colorado State University
Department of Elec. and Comp. Engineering
Fort Collins, CO 80523, USA

ABSTRACT

Compressed sensing theory suggests that successful inversion of an image of the physical world from its modal parameters can be achieved at measurement dimensions far lower than the image dimension, provided that the image is sparse in an *a priori known* basis. The *assumed* basis for sparsity typically corresponds to a gridding of the parameter space, e.g., an DFT grid in spectrum analysis. However, in reality no physical field is sparse in the DFT basis or in an a priori known basis. No matter how finely we grid the parameter space the sources may not lie in the center of the grid cells and there is always mismatch between the assumed and the actual bases for sparsity. In this paper, we study the sensitivity of compressed sensing (basis pursuit to be exact) to mismatch between the assumed and the actual sparsity bases. Our mathematical analysis and numerical examples show that the performance of basis pursuit degrades considerably in the presence of basis mismatch.

Index Terms— Compressed sensing, image inversion, image reconstruction, sensitivity to basis mismatch, sparse recovery.

1. INTRODUCTION

The recent advent of compressed sensing and sparse recovery methods (cf. [1]–[3]) has created a great deal of enthusiasm among the signal processing community, as it suggests that reconstructing and even inverting high dimensional images (e.g., a radar/sonar return) can be performed from far fewer measurements than the image dimension, provided that the image is sparse in an *a priori known* basis.

The sparsity basis, *assumed* in the compressed sensing procedure, varies with application but it typically corresponds to a gridding of the parameter space. For example, in radar/sonar imaging, the basis is usually taken to be a DFT basis constructed for resolution of $2\pi/N$, with N a window length, array length, or pulse-to-pulse processing length (cf. [4],[5]).

The work of R. Calderbank and Y. Chi is supported in part by NSF under grants DMS-0701226 and CCF-0916314, by ONR under grant N00173-06-1-G006, and by AFOSR under grant FA9550-05-1-0443. The work of A. Pezeshki is supported by the NSF under grant CCF-0916314.

However, in reality no physical field is sparse in the DFT basis or in an a priori known basis and in fact the main goal in image inversion is to *identify* the modal structure of the image. No matter how large the size N of the grid is, the actual field will not place its sources on the center of the grid points $\{2\pi n/N\}$ in frequency, or on the center of the grid points in delay-Doppler-wavenumber. This means the image is actually *not sparse* in the DFT basis or the basis defined by the grid. In fact any source that lies between two grid cells will spill non-zero values into all cells, with the amplitude of the spillage following a Lanczos kernel, decaying as $1/f$, where f is frequency or wavenumber. This spillage makes the image non-sparse or non-compressible in the assumed basis.

This observation raises the following question. *What is the sensitivity of compressed sensing for image inversion to mismatch between the assumed basis for sparsity and the actual basis in which the image is sparse?* In order to frame this question more precisely, let us begin with two models for an image $\mathbf{s} \in \mathbb{C}^N$. In the mathematical model, to be *assumed* in the compressed sensing procedure, the image is composed as $\mathbf{s} = \mathbf{\Psi}_0\mathbf{x}$, where $\mathbf{\Psi}_0 \in \mathbb{C}^{N\times N}$ is known (e.g., the N point DFT matrix) and $\mathbf{x} \in \mathbb{C}^N$ is a sparse or compressible vector of field parameters that compose the image as a linear combination of columns of $\mathbf{\Psi}_0$. But, as a matter of fact, the image $\mathbf{s}$ is composed by the physics as $\mathbf{s} = \mathbf{\Psi}_1\boldsymbol{\theta}$, where $\mathbf{\Psi}_1 \in \mathbb{C}^{N\times N}$ and the field parameter vector $\boldsymbol{\theta}$ is sparse. Typically $\mathbf{\Psi}_1$ is determined by frequency, wavenumber, delay, and/or doppler parameters that are *unknown* a priori. More importantly, these parameters do *not* lie exactly on the gridding points of $\mathbf{\Psi}_0$, e.g. a DFT matrix or an identity matrix. So $\mathbf{\Psi}_0 \neq \mathbf{\Psi}_1$. We call this basis mismatch, and note that it is present in all imaging problems, no matter how large N is, or equivalently how fine-grained the gridding procedure is.

If we invert each model for the corresponding parameter vectors $\mathbf{x} = \mathbf{\Psi}_0^{-1}\mathbf{s}$ and $\boldsymbol{\theta} = \mathbf{\Psi}_1^{-1}\mathbf{s}$ we will obtain the coordinate transformation $\mathbf{x} = \mathbf{\Psi}\boldsymbol{\theta}$, where $\mathbf{\Psi} = \mathbf{\Psi}_0^{-1}\mathbf{\Psi}_1 \in \mathbb{C}^{N\times N}$. If $\mathbf{s}$ is sparse in $\mathbf{\Psi}_1$, as is typical in spectrum analysis, beamforming, and radar imaging, then the field parameters $\boldsymbol{\theta}$ will be sparse in the identity basis, denoted by $\mathbf{I}$. The field parameters $\mathbf{x} = \mathbf{\Psi}\boldsymbol{\theta}$ will be sparse in the $\mathbf{\Psi}$ basis, *but not in the identity basis*. The question is, "what is the consequence of assuming that $\mathbf{x}$ is sparse in $\mathbf{I}$, when in fact $\mathbf{x}$ is only sparse

in an *unknown* basis $\mathbf{\Psi}$, which is determined by the mismatch between $\mathbf{\Psi}_0$ and $\mathbf{\Psi}_1$?"

We answer this questions by deriving bounds on the ℓ_1-norms of errors in recovering the actual parameter vector $\boldsymbol{\theta}$ associated with the unknown basis $\mathbf{\Psi}_1$ and the hypothesized parameter vector associated with the assumed basis $\mathbf{\Psi}_0$ from compressed sensing measurements of $\mathbf{s}$ using basis pursuit. We refer to recovering $\boldsymbol{\theta}$ as image inversion, as we try to invert $\mathbf{s}$ for its true sparse parameters $\boldsymbol{\theta}$, and we refer to recovering $\mathbf{x}$ as image reconstruction as $\mathbf{s}$ can be recomposed as $\mathbf{s} = \mathbf{\Psi}_0\mathbf{x}$ from the estimate of $\mathbf{x}$. We show that the upper bounds for the ℓ_1 errors for inversion and reconstruction grow linearly with the image (or grid) dimension N and the mismatch level between $\mathbf{\Psi}$ and $\mathbf{I}$. We substantiate our mathematical analysis by numerical examples that demonstrate a considerable performance degradation for image inversion/reconstruction using basis pursuit. In image inversion, the inaccuracy persists even when the number of compressed sensing measurements is increased to the full image dimension. It is this mismatch problem that moderates our enthusiasm for compressed sensing as a high resolution image inversion principle, at least for problem sizes typical in radar/sonar and spectrum analysis.

This paper is a summary of results. We have omitted the proofs, and derivations have been shortened or left out entirely. A comprehensive treatment with proofs is presented in [6]. Additional numerical examples can be found in [7].

Remark: This paper is concerned with the effect of basis mismatch and not with the effect of perturbations in the compressed sensing measurement matrix with respect to a so-called RIP matrix. The latter problem is considered in [8].

2. BASIS MISMATCH IN COMPRESSED SENSING

The compressed sensing observation vector $\mathbf{y}$ is given by

$$\mathbf{y} = \mathbf{\Phi s} = (\mathbf{\Phi\Psi}_0)\mathbf{x} \triangleq \mathbf{Ax} \tag{1}$$

where $\mathbf{\Phi} \in \mathbb{C}^{M\times N}$ is the measurement matrix (typically a matrix with i.i.d. Gaussian or i.i.d Bernoulli entries), and M is the number of measurements.[1] We define $\mathbf{A} = \mathbf{\Phi\Psi}_0 \in \mathbb{C}^{M\times N}$ as the compressed sensing measurement matrix with respect to $\mathbf{x}$ and, without loss of generality, only deal with $\mathbf{A}$ and $\mathbf{\Psi}$ in our discussions.

If $\mathbf{A} = \mathbf{\Phi\Psi}_0$ satisfies the restricted isometry property (RIP) (cf. [9],[10]) with $\delta_{2k}^{\mathbf{A}} < \sqrt{2} - 1$ for $2k$-sparse signals, the solution to the so called basis pursuit (BP) problem

$$\mathbf{x}^* = \arg\min_{\mathbf{x}} \|\mathbf{x}\|_1 \quad s.t. \quad \mathbf{y} = \mathbf{Ax}. \tag{2}$$

obeys $\|\mathbf{x}^* - \mathbf{x}\|_1 \leq C_0\|\mathbf{x} - \mathbf{x}_k\|_1$, where $\mathbf{x}_k$ is the best k-term approximation of $\mathbf{x}$, and C_0 depends only on the RIP constant $\delta_{2k}^{\mathbf{A}}$.

In the matched case where $\mathbf{\Psi}_0$ coincides with $\mathbf{\Psi}_1$, $\mathbf{\Psi} = \mathbf{\Psi}_0^{-1}\mathbf{\Psi}_1$ reduces to $\mathbf{I}$ and $\mathbf{x} = \boldsymbol{\theta}$ is sparse in the $\mathbf{I}$ basis. If $\boldsymbol{\theta}$ is k-sparse, the best k-term approximation error $\|\mathbf{x} - \mathbf{x}_k\|_1$ will be zero and the BP solution $\mathbf{x}^*$ to $\mathbf{x}$ will be exact.

However, in the mismatched case where $\mathbf{\Psi}_0 \neq \mathbf{\Psi}_1$, $\mathbf{x} = \mathbf{\Psi}\boldsymbol{\theta}$ is actually sparse in the $\mathbf{\Psi}$ basis, rather than the $\mathbf{I}$ basis. The question is, "what is the consequence of minimizing $\|\mathbf{x}\|_1$ under the constraint $\mathbf{y} = \mathbf{Ax}$ for image inversion and image reconstruction,[2] when in fact the correct problem is to minimize $\|\boldsymbol{\theta}\|_1$ under the constraint $\mathbf{y} = \mathbf{A\Psi}\boldsymbol{\theta}$ where $\mathbf{A} = \mathbf{\Phi\Psi_0}$?"

3. PERFORMANCE DEGRADATION IN MISMATCH

We start by analyzing the effect of basis mismatch on the best k-term approximation ℓ_1 error $\|\mathbf{x} - \mathbf{x}_k\|_1$, which is central to arguing for the the accuracy of the BP solution. Here, we derive bounds for $\|\mathbf{x} - \mathbf{x}_k\|_1$ in terms of the mismatch level between $\mathbf{\Psi}$ and $\mathbf{I}$ and the image dimension N. We then use these bounds to show the effect of basis mismatch on the ℓ_1 errors in recovering $\mathbf{x}$ and $\boldsymbol{\theta}$.

Let us express the mismatched basis $\mathbf{\Psi} \in \mathbb{C}^{N\times N}$ as $\mathbf{\Psi} = \mathbf{I} + \mathbf{E}$, where $\mathbf{E}$ is a perturbation matrix with respect to the identity basis and $\mathbf{x} = \mathbf{\Psi}\boldsymbol{\theta}$. Let $\mathbf{x}_k$ and $\boldsymbol{\theta}_k$ denote the best k-term approximations to $\mathbf{x}$ and $\boldsymbol{\theta}$ respectively, that is

$$\mathbf{x}_k = \underset{\mathbf{z}\in\Sigma_k}{\operatorname{argmin}} \|\mathbf{x} - \mathbf{z}\|_1 \quad \text{and} \quad \boldsymbol{\theta}_k = \underset{\mathbf{z}\in\Sigma_k}{\operatorname{argmin}} \|\boldsymbol{\theta} - \mathbf{z}\|_1$$

where $\Sigma_k = \{\mathbf{z} \in \mathbb{C}^N : |T_{\mathbf{z}}| \leq k\}$ and $T_{\mathbf{z}}$ is the support of $\mathbf{z}$.

Theorem 1 (k-term approximation error): Let $\mathbf{\Psi} = \mathbf{I} + \mathbf{E}$ and $\mathbf{x} = \mathbf{\Psi}\boldsymbol{\theta}$. Let $1 \leq p, q \leq \infty$ and $1/p + 1/q = 1$. If the rows of $\mathbf{E}$ are bounded as $\|\mathbf{e}_m\|_p \leq \beta$ for $1 \leq m \leq N$, then

$$|\|\mathbf{x} - \mathbf{x}_k\|_1 - \|\boldsymbol{\theta} - \boldsymbol{\theta}_k\|_1| \leq (N-k)\beta\|\boldsymbol{\theta}\|_q. \tag{3}$$

The bound is achieved when the entries of $\mathbf{E}$ satisfy

$$e_{mn} = \pm\beta \cdot e^{j\arg(\theta_m)}e^{-j\arg(\theta_n)} \cdot (|\theta_n|/\|\boldsymbol{\theta}\|_q)^{q/p} \tag{4}$$

for $n \in T_{\boldsymbol{\theta}}$ and $1 \leq m \leq N$.

When $\boldsymbol{\theta}$ is exactly k-sparse in $\mathbf{I}$, i.e., $\boldsymbol{\theta} = \boldsymbol{\theta}_k$, (3) reduces to

$$\|\mathbf{x} - \mathbf{x}_k\|_1 \leq (N-k)\beta\|\boldsymbol{\theta}\|_q, \tag{5}$$

which shows that the upper bound on the best k-term approximation ℓ_1 error $\|\mathbf{x} - \mathbf{x}_k\|_1$ is linearly increasing in N, β and $\|\boldsymbol{\theta}\|_q$, and linearly decreasing in k.

Theorem 2 (k-term approximation worst-case error): Let $\mathbf{\Psi} = \mathbf{I} + \mathbf{E}$ and $\mathbf{x} = \mathbf{\Psi}\boldsymbol{\theta}$. Let $1 \leq p, q \leq \infty$ and $1/p + 1/q = 1$. If the rows of $\mathbf{E}$ are lower bounded as $\|\mathbf{e}_m\|_p \geq \eta$, then

$$\max_{\mathbf{E}:||\mathbf{e}_m||_p\geq\eta} \|\mathbf{x} - \mathbf{x}_k\|_1 \geq \|\boldsymbol{\theta} - \boldsymbol{\theta}_k\|_1 + (N-k)\eta\|\boldsymbol{\theta}\|_q. \tag{6}$$

[1] In this paper, we consider a noise-free observation model for simplicity. However, all of our results can be easily extended to the noisy case (cf. [6].)

[2] In image reconstruction, the objective is to recompose $\mathbf{s}$ in the assumed basis $\mathbf{\Psi}_0$ and hence we are interested in estimating $\mathbf{x}$ with the BP solution $\mathbf{x}^*$. In image inversion, we wish to estimate the true parameter vector $\boldsymbol{\theta}$. But, since the sparsity basis $\mathbf{\Psi}_1$ is unknown, we resort to solving the mismatched BP problem and we have no choice but to take $\mathbf{x}^*$ as an estimate of $\boldsymbol{\theta}$.

Remark: When $q = 1$ and $p = \infty$, Theorems 1 and 2 hold for $|e_{mn}| \leq \beta$ and $|e_{mn}| \geq \eta$, respectively, with $n \in T_{\boldsymbol{\theta}}$.

Fig. 1 illustrates the interplay between Theorems 1 and 2 for $q = 1$, when $\eta \leq |e_{mn}| \leq \beta$ for $n \in T_{\boldsymbol{\theta}}$ and $\boldsymbol{\theta}$ is k-sparse. The outer diamond has radius $A(\beta) = (N-k)\beta$ and corresponds to the upper bound in Theorem 1. The inner diamond, with radius $A(\eta)$, corresponds to Theorem 2 and indicates that there exists a mismatched basis $\boldsymbol{\Psi} = \mathbf{I} + \mathbf{E}$ for which the best k-term approximation $\mathbf{x}_k$ lies between the two diamonds, prohibiting us from giving any meaningful guarantee about the accuracy of the BP solution based on the k-term approximation bound.

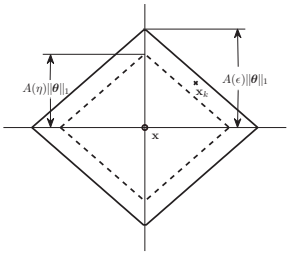

Fig. 1. Confidence diamonds for $\mathbf{x}_k$ when $\eta \leq |e_{mn}| \leq \beta$ for $n \in T_{\boldsymbol{\theta}}$ and $\boldsymbol{\theta}$ is k-sparse.

Theorem 3 (image reconstruction error): Let $\mathbf{A}$ be fixed and satisfy $\delta_{2k}^{\mathbf{A}} < \sqrt{2} - 1$. Let $1 \leq p, q \leq \infty$ and $1/p + 1/q = 1$. If the rows of $\mathbf{E}$ satisfy $\|\mathbf{e}_m\|_p \leq \beta$, then the reconstruction error $\|\mathbf{x}^* - \mathbf{x}\|_1$ is bounded below

$$\|\mathbf{x}^* - \mathbf{x}\|_1 \leq C_0 \|\boldsymbol{\theta} - \boldsymbol{\theta}_k\|_1 + C_0 (N-k)\beta \|\boldsymbol{\theta}\|_q. \quad (7)$$

Theorem 4 (image inversion error): Let $\mathbf{A}$ be fixed and satisfy $\delta_{2k}^{\mathbf{A}} < \sqrt{2} - 1$. Let $1 \leq p, q \leq \infty$ and $1/p + 1/q = 1$. If the entries of $\mathbf{E}$ satisfy $\|\mathbf{e}_m\|_p \leq \beta$, then for noiseless recovery (2), the inversion error is bounded as below

$$\|\mathbf{x}^* - \boldsymbol{\theta}\|_1 \leq C_0 \|\boldsymbol{\theta} - \boldsymbol{\theta}_k\|_1 + [C_0(N-k) + N]\, \beta \|\boldsymbol{\theta}\|_q. \quad (8)$$

The upper bounds on $\|\mathbf{x}^* - \mathbf{x}\|_1$ and $\|\mathbf{x}^* - \boldsymbol{\theta}\|_1$ are both linearly increasing in the image (or grid) dimension N and in the mismatch level β. The bounds are linearly decreasing in k. The maximum allowable value for k, for which the BP bounds still hold, depends on the measurement matrix $\mathbf{A}$. For $\mathbf{A} \in \mathbb{R}^{M \times N}$ to be RIP with constant $\delta_{2k}^{\mathbf{A}} < \sqrt{2} - 1$ we typically require $M = \mathcal{O}\left(k \log(N/k)\right)$.

4. NUMERICAL EXAMPLES

In all the examples, the measurement matrix $\mathbf{A}$ is generated with i.i.d Gaussian entries and corresponding dimension.

Example 1. Let $\boldsymbol{\Psi}_0 = \mathbf{I}$ be the sparsity basis assumed in the compressed sensing procedure and let $\boldsymbol{\Psi}_1 = \mathbf{I} + \epsilon \mathbf{J}$ be the actual sparsity basis, where $\mathbf{J}$ is the matrix with every entry 1. Then the mismatched basis is $\boldsymbol{\Psi} = \boldsymbol{\Psi}_0^{-1} \boldsymbol{\Psi}_1 = \mathbf{I} + \epsilon \mathbf{J}$. Assume that the true parameter vector $\boldsymbol{\theta}$ is a sparse vector in which all nonzero entries are equal to one and the positions of the nonzero entries are uniformly distributed. This example amounts to the worst case mismatch scenario in Theorem 1, with $q = 1$, where the bound becomes tight. In this case, $\|\mathbf{x}\|_1 = (1 + N\epsilon)\|\boldsymbol{\theta}\|_1$, then the normalized error bound can be written as following Theorem 3

$$\frac{\|\mathbf{x}^* - \mathbf{x}\|_1}{\|\mathbf{x}\|_1} \leq \frac{C_0}{1 + N\epsilon} \frac{\|\boldsymbol{\theta} - \boldsymbol{\theta}_k\|_1}{\|\boldsymbol{\theta}\|_1} + C_0 \frac{(N-k)\epsilon}{1 + N\epsilon}. \quad (9)$$

Fig. 2 shows the normalized ℓ_1 error $\|\mathbf{x}^* - \mathbf{x}\|_1 / \|\mathbf{x}\|_1$ as a function of the mismatch parameter ϵ for dimensions $N = 512$, $M = 64$ and sparsity level $k = 10$ for $\boldsymbol{\theta}$. We observe that even for moderate amounts of mismatch the normalized ℓ_1 error is considerable. When the mismatch level ϵ goes to infinity, the normalized error bound converges to $C_0\left(\frac{N-k}{N}\right)$. In Fig. 2 (b), the error curve becomes flat when ϵ is above $\mathcal{O}(10^{-2})$.

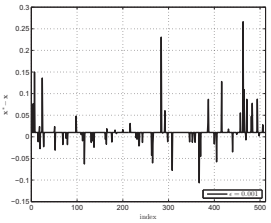

(a)

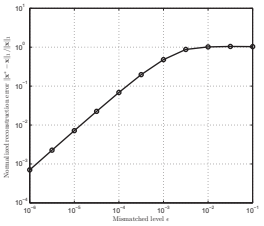

(b)

Fig. 2. (a) $\mathbf{x}^* - \mathbf{x}$ for $\epsilon = 0.001$. (b) $\|\mathbf{x}^* - \mathbf{x}\|_1 / \|\mathbf{x}\|_1$ vs. ϵ.

Example 2. Here, we assume that the image $\mathbf{s}$ is a single tone (a 1-sparse signal) with an unknown frequency. The actual sparsity basis $\boldsymbol{\Psi}_1$ is a matrix whose n-th column is mismatched in frequency by $0 \leq \Delta\theta < \frac{2\pi}{N}$ with respect to the n-th column of the N-point DFT matrix, which the compressed sensing procedure takes as the sparsity basis $\boldsymbol{\Psi}_0$. The rest of the columns of $\boldsymbol{\Psi}_1$ and $\boldsymbol{\Psi}_0$ are assumed to be identical. The mismatched basis $\boldsymbol{\Psi} = \boldsymbol{\Psi}_0^{-1} \boldsymbol{\Psi}_1$ can be written as

$$\boldsymbol{\Psi} = \mathbf{I} + (\mathbf{U}^n \boldsymbol{\delta}) \otimes \mathbf{I}(n)^T \triangleq \mathbf{I} + \mathbf{E} \quad (10)$$

where $\mathbf{U}^n$ is an upper shift matrix by n, $\mathbf{I}(n)$ is the n-th column of $\mathbf{I}$, $\otimes$ is Kronecker product, $\boldsymbol{\delta} = [\delta_0 - 1, \delta_1, \ldots, \delta_{N-1}]^T$, and δ_m's are samples of the Lanczos kernal at $\omega_m = \left(\Delta\theta - \frac{2\pi m}{N}\right)$, that is,

$$\delta_m = \frac{1}{N} e^{-j\omega_m\left(\frac{N-1}{2}\right)} \frac{\sin(N\omega_m/2)}{\sin(\omega_m/2)}. \quad (11)$$

As $\Delta\theta$ increases from 0 to $0.5 \cdot 2\pi/N$, the entries of the mismatch matrix $|e_{mn}|$ increases. When $\Delta\theta = 0.5 \cdot 2\pi/N$, the entries δ_k, $k > 0$ are the peak values of the sidelobes of the Lanczos kernel, which correspond to the worst frequency mismatch.

Fig. 3 (a) shows the normalized ℓ_1 error $\|\mathbf{x} - \mathbf{x}_k\|_1 / \|\mathbf{x}\|_1$ for different frequency mismatch levels $\Delta\theta$ and different values for k, when the single tone is located off of the $(n = 10)$-th DFT frequency in the $(N = 512)$-point DFT grid. The

plot shows that the normalized best k-term approximation error is considerable even at moderate mismatch levels. Let the number of measurement $M = 64$. Fig. 3 (b) shows the reconstructed signal superimposed on the actual tone for different mismatch levels. The inaccuracy is noticeable for 25% and 50% frequency mismatch. Similar results (cf. [6]) were obtained when this example was run with dimensions $(N = 512, M = 100)$, $(N = 1024, M = 200)$, and $(N = 2048, M = 400)$. In all experiments, the normalized ℓ_1 reconstruction error $\|\mathbf{x}^* - \mathbf{x}\|_1/\|\mathbf{x}\|_1$ exhibited almost-linear growth with increase in $\Delta\theta$. The plots are omitted due to lack of space.

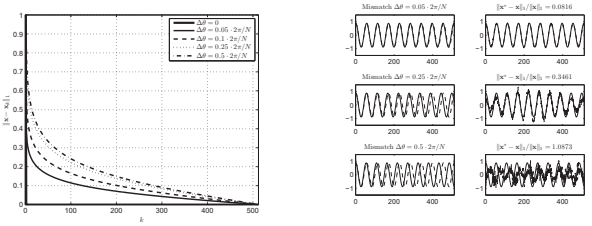

(a) (b)

Fig. 3. (a) $\|\mathbf{x} - \mathbf{x}_k\|_1/\|\mathbf{x}\|_1$ vs. $\Delta\theta/(2\pi/N)$ for various k. (b) Mismatched tones (left) and the reconstructed tones (right) superimposed on the actual tone.

Example 3. We now present a modal analysis example where we wish to invert an image for its mode amplitudes. The compressed sensing procedure assumes that the frequency modes coincide with the DFT frequencies, located at $2\pi n/N$ points with $N = 64$, but the actual signal has modes that are off the centers of the DFT grid cells. The actual frequency modes and their amplitudes are $(9.25 \cdot 2\pi/N, 1)$, $(9.75 \cdot 2\pi/N, 1)$, $(20 \cdot 2\pi/N, .5)$, and $(45 \cdot 2\pi/N, .2)$ with randomly generated phases. Fig. 4 (a) shows the location of the modes on the unit circle. The heights of the bars represent the mode amplitudes. The estimate for $\boldsymbol{\theta}$, obtained by solving the mismatched BP problem, is plotted in Fig. 4 (b) for measurement budget $M = N/4 = 16$. The plot shows that compressed sensing fails to recover the modes correctly in the presence of mismatch. The inaccuracy persists even when the number of measurements is increased to the full image dimension. The reader is referred to [7] for additional numerical evidence, including noisy cases, and comparisons with linear prediction and matched filtering.

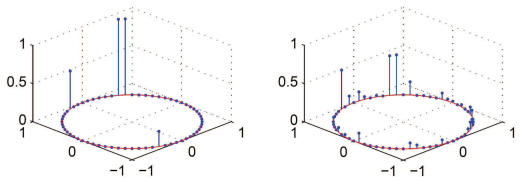

(a) Actual (b) Mismatch; $M = 16$

Fig. 4. Performance degradation of compressed sensing for modal analysis in the presence of basis mismatch.

5. CONCLUSIONS

The theory of compressed sensing suggests that compressed recording of an image has manageable consequences for image inversion/reconstruction, provided the image is sparse in an a priori known basis, typically associated with a gridding of the parameter space. But no physical field is sparse in a basis defined by a regular grid in delay, doppler, frequency, and/or wavenumber and there is always mismatch between the assumed basis for sparsity and the actual sparsity basis. Our mathematical analysis and numerical examples indicate that the performance of compressed sensing for reconstructing a sparse physical field degrades considerably in the presence of basis mismatch, even when the assumed basis corresponds to an extremely fine-grained discretization of the parameter space. The conclusion at this point is that for high resolution spectrum analysis, beamforming, or radar/sonar imaging, where the problem is to identify a small number of modal parameters, compressed sensing requires more study.

6. REFERENCES

[1] E. J. Candés, "Compressive sampling," *Proc. Int. Congress Math.*, vol. 3, pp. 1433–1452, 2006.

[2] D. L. Donoho, "Compressed sensing," *IEEE Trans. Inform. Theory*, vol. 52, no. 4, pp. 1289–1306, 2006.

[3] R. Baraniuk, "Compressive sensing," *IEEE Signal Processing Magazine*, vol. 24, no. 4, pp. 118–121, 2007.

[4] M. A. Herman and T. Strohmer, "High-resolution radar via compressed sensing," *IEEE Trans. Signal Processing*, to appear 2009.

[5] A. Gurbuz, J. McClellan, and V. Cevher, "A compressive beamforming method," in *Proc. ICASSP'08*, Las Vegas, NV, Apr. 2008, pp. 2617–2620.

[6] Y. Chi, A. Pezeshki, L. L. Scharf, and R. Calderbank, "Sensitivity to basis mismatch of compressed sensing," *preprint*, Aug. 2009.

[7] Y. Chi, L. L. Scharf, A. Pezeshki, and R. Calderbank, "Sensitivity to basis mismatch of compressed sensing for spectrum analysis and beamforming," in *2009 Workshop on Defence Applications of Signal Processing (DASP)*, Lihue, HI, Sep. 2009.

[8] M. A. Herman and T. Strohmer, "General deviants: An analysis of perturbations in compressed sensing," arXiv:0907.2955v1.

[9] E. J. Candés and T. Tao, "Decoding by linear programming," *IEEE Trans. Inform. Theory*, vol. 51, pp. 4203–4215, Dec. 2005.

[10] E. J. Candés, "The restricted isometry property and its implications for compressed sensing," *Académie des Sciences*, vol. 1, no. 346, pp. 589– 592, 2008.